Available online www.jsaer.com

Journal of Scientific and Engineering Research, 2016, 3(6):93-100

Research Article

ISSN: 2394-2630
CODEN(USA): JSERBR

Finite Element Simulation of Land Subsidence under Seasonal Pumping and Dewatering

Taher Baher Talari

Civil Engineering Department, University of Mohaghegh Ardabili, Ardabil, Iran

Abstract Land subsidence is a phenomenon that involves the lowering or settling of the earth's surface due to various factors. In recent years, it has been proven that Kerman Province subsidence in Iran is due to extensive ground water withdrawal. A decrease in ground water level would causes an increase in effective stresses at clay layers which results consolidation of lower layers. In this research it is assumed that the water table level surface oscillate horizontally due to a group well pumping. This oscillation of water table for farming in various seasons of the year would produce cyclic loading. For modelling of any oscillation of water table, correlation between classical parameters, and parameters for numerical analysis was developed. A simple correlation between these parameters was found. Based on the model prediction the variation of settlement in the ground can be seen. The results show good comparison with field data.

Keywords Punica granatum L.; Quercetin: Luteolin; Kaempferol: Natural dyes; dyeing, mordant, LC-MS

Introduction

In the recent years, land subsidence in many part of the world including Iran has become a major consideration. The considered land subsidence in this research is mainly due to excessive ground water withdrawal which causes differential settlement and earth fissures. It has been conformed that land subsidence in Kerman Province in Iran is due to consolidation of soil layers, caused by extensive groundwater withdrawal for agriculture development which introduced large land subsidence and earth fissures [1].

A semi-complete field investigation was first undertaken by Rahmanian (1986) [1]. His results show that in the Kerman Province subsidence and earth fissures were related only to heavy pumping of the ground water and subsequent continued decline in the water table. Later this investigation was continued by Toufigh and Shafeiei (1995 and 1996), and Toufigh and Q'marsi (2002) and Ouria and Toufigh (2010). They provide a prediction model in order to simulate the future settlement [2-5].

In this research, it is assumed that the water table level surface drops horizontally due to a group well pumping. In the case of seasonal pumping the water level drops to a certain depth and then returns to previous level for the time of no pumping. This oscillation of water table would impose cyclic loading on the layers of clays below the water table surface. In this study a site under cyclic loading was modeled based on finite element formulation. In order to simulate and predict such phenomenon in a given group wells, a fully coupled finite element model is developed. In order to verify the finite element model, the annual settlement rate obtained from the finite element model was compared with the results observed in the field. Formulation of finite element was based on Biot's three-dimensional consolidation theory. As excess effective stress, due to water withdrawal in whole scale is small, behavior of soil skeleton was assumed to be elastic, but it should be noted that pore water pressure variation is still function of time, depth and other properties and boundary conditions.

Cyclic loading resulted from seasonal pumping

Cyclic loading can be produced by oscillation of water table in different seasons of the year. In static loading the derivative value of the mean total stresses due to time is very small and can be neglected, but for time dependent loading this assumption will not be correct. In order to consider the effect of cyclic loading, this can be substituted by superimposed static loading. In Figure 1 it is shown the water table drops a certain depth due to large number of pumps in a given region and stays constant for a period of time, then pumps stop for the equivalent of the first period. This is an example of seasonal pumping of water for spring and summer and no pumping for fall and winter. This is exactly what is happening at agricultural regions in Kerman Province. The above effect would introduce as would explain latter in this paper a cyclic loading on the soils below the water table.

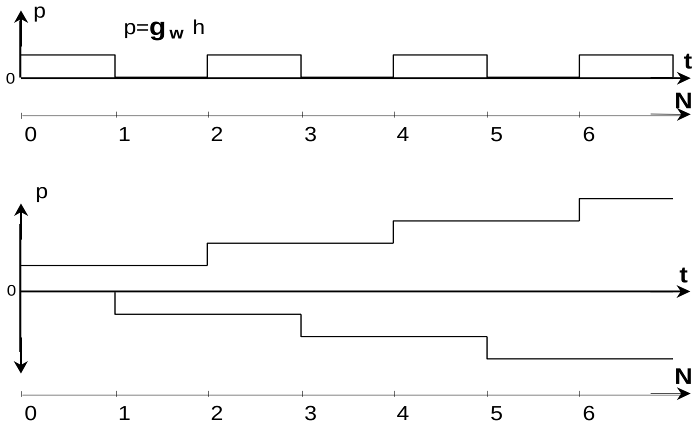

Figure 1: Cyclic Loading and Proposed Equivalent Superimposed Static Loading

In order to model the actual loading on the soil, it can be demonstrated by adopting a superimposing static load technique as shown in lower part of Figure 1. Based on above the degree of consolidation for any cyclic loading can be write [6-7]:

$$U_{c(N)} = (-1)^N \sum_{i=1}^{N} (-1)^i U_{(i.T/2)} \tag{1}$$

Which U is degree of consolidation, Uc, degree of consolidation under cyclic loading, T is cyclic period and N is number of half cycle.

The above relationship is true if the coefficient of consolidation during loading and unloading stay constant. In order word soil behave as elastic material. In the condition of inelastic behavior, the coefficient of consolidation increases with the increase number of cycles. This would stay constant when the soil reaches complete consolidation.

This means that when a normally consolidated soil experience a large number of cyclic loading it would behave more like an elastic material. Therefore, for inelastic behavior, amount of settlement, pour water pressure and final degree of consolidation would be equal to over consolidated elastic condition. For analyses of inelastic behavior every single cycle would process independently and assumed that effect of each cycle loading would not influence the other cycle effect, and only coefficient of consolidation can be varied. For each cycle the coefficient of consolidation can be computed as [6]:

$$c_{vN} = c_v . f(N, \beta) = c_v \frac{1-(1-\beta)^{\frac{N+1}{2}}}{\beta} \tag{2}$$

$$\beta = \frac{c_v(nc)}{c_v(oc)}$$

By assumption of independent effect of loading on each cycle, this would introduce an error. This error shows negative pore pressure in the next cycle, which is no loading condition. The negative pore water at end of loading cycle can be computed by Equation 3.

$$u_{e(z,t+\Delta t)} = -\Delta P + u_{e(z,t-\Delta t)} \tag{3}$$

At the period of no loading if the negative pore water pressure dose not dissipate, this could create an extra compressive effective stress on the system. Therefore, this error would influence on the computing of the final settlement which usually is smaller than the actual settlement. Computing of final settlement based on inelastic behavior contains some error. This error is zero at end of first half cycle and increases with the number of cycles. Now based of variation shape of errors the computed settlement of the system can be modified and finally obtain the actual settlement of soil.

Finite element formulation

The basic formulation presented here is based on Biot's consolidation theory. In the theory of Biot the soil skeleton treated as a porous elastic solid and the laminar pore fluid are coupled by the conditions of compressibility and of continuity.

The formulation was conducted in asymmetric cylindrical coordinate system. When water is pumped out from the aquifer through wells, both radial and vertical flow can take place, which are symmetric. In order to simulate this condition by finite element the exact behavior should be achieved by actual mathematical equations. For each reason Biot's governing equation was selected; which is:

$$C_r\left(\frac{\partial^2 u_e}{\partial r^2} + \frac{1}{r}\frac{\partial u_e}{\partial r}\right) + C_z\frac{\partial^2 u_e}{\partial z^2} = \frac{\partial u_e}{\partial t} - \frac{\partial P}{\partial t} \tag{4}$$

where u_e = excess pore water pressure,

P = mean total stress,

z and r = axial and radial directions,

t = time, and

C_r, C_z = coefficient of consolidation in radial and axial directions, respectively.

The equilibrium equation with assumption of zero volumetric force, can be written as follows:

$$\begin{aligned} \frac{\partial \sigma'_r}{\partial r} + \frac{\partial \tau_{rz}}{\partial z} + \frac{\partial u_e}{\partial r} &= 0 \\ \frac{\partial \tau_{rz}}{\partial r} + \frac{\partial \sigma'_z}{\partial z} + \frac{\partial u_e}{\partial z} &= 0 \end{aligned} \tag{5}$$

The stress-strain relations for such condition can be written as follows:

$$\begin{Bmatrix} \sigma'_r \\ \sigma'_z \\ \tau_{rz} \\ \sigma'_\theta \end{Bmatrix} = \frac{E(1-\upsilon)}{(1+\upsilon)(1-2\upsilon)} \times \begin{bmatrix} 1 & \frac{\upsilon}{1-\upsilon} & 0 & \frac{\upsilon}{1-\upsilon} \\ \frac{\upsilon}{1-\upsilon} & 1 & 0 & \frac{\upsilon}{1-\upsilon} \\ 0 & 0 & \frac{1-2\upsilon}{2(1-\upsilon)} & 0 \\ \frac{\upsilon}{1-\upsilon} & \frac{\upsilon}{1-\upsilon} & 0 & 1 \end{bmatrix} \begin{Bmatrix} \varepsilon_r \\ \varepsilon_z \\ \gamma_{rz} \\ \varepsilon_\theta \end{Bmatrix} \tag{6}$$

where E = modules of elasticity,

υ = Poisson's ratio,

σ' = effective stress,
ε = strain, and

$$\begin{Bmatrix} q_r \\ q_z \end{Bmatrix} = \frac{1}{\gamma_w} \begin{bmatrix} K_r & 0 \\ 0 & K_z \end{bmatrix} \begin{Bmatrix} \frac{\partial u_e}{\partial r} \\ \frac{\partial u_e}{\partial z} \end{Bmatrix} \quad (7)$$

where q_r, q_z = volumetric flow rates per unit area into and out of the element,

K_r, K_z = Coefficient of permeability in redial and axial directions, respectively.

For fully saturated soil and incompressible fluid condition, outflow from an element of soil equals the reduction in volume of element. Hence:

$$\frac{\partial q_r}{\partial r} + \frac{\partial q_z}{\partial z} = \frac{d}{dt}\left(\frac{\partial u}{\partial r} + \frac{\partial v}{\partial z}\right) \quad (8)$$

where u and v = displacements in r and z directions, respectively.
Combining Eqns (4) and (5):

$$\frac{K_r}{\gamma_w}\frac{\partial^2 u_e}{\partial r^2} + \frac{K_z}{\gamma_w}\frac{\partial^2 u_e}{\partial z^2} + \frac{d}{dt}\left(\frac{\partial u}{\partial r} + \frac{\partial v}{\partial z}\right) = 0 \quad (9)$$

As usual in a displacement method σ, ε are eliminated in terms of u, v so that the final coupled variables are u, v, u_e.

These are now discretized in the normal way:

$$u = Xu$$
$$v = Xv \quad (10)$$
$$u_e = Xu_e$$

where X is the vector of shape function.
When discretization and the Galerkin process are completed, Equations 5 and 9 lead to the pair of equilibrium and continuity equations, which are:

$$KM_r + Cu_e = F$$
$$C^T \frac{dr}{dt} - KPu_e = 0 \quad (11)$$

where, for a four-nodded element,

$$r = \{u_1, \; v_1, \; u_2, \; v_2, \; u_3, \; v_3, \; u_4, \; v_4\}^T$$
$$u_e = \{u_{e1}, \; u_{e2}, \; u_{e3}, \; u_{e4}\}^T \quad (12)$$

KM is the elastic stiffness matrix and is

$$KM = \iint B^T DBrdrdz \quad (13)$$

where, B = AX,
X =vector of shape function, and

$$A = \begin{Bmatrix} \frac{\partial}{\partial r} & 0 \\ 0 & \frac{\partial}{\partial r} \\ \frac{\partial}{\partial z} & \frac{\partial}{\partial r} \\ \frac{1}{r} & 0 \end{Bmatrix} \quad (14)$$

KP is the fluid stiffness matrix is

$$KP = \iint \left(C_r \frac{\partial X_i}{\partial r} \frac{\partial X_j}{\partial r} + C_z \frac{\partial X_i}{\partial z} \frac{\partial X_j}{\partial z} \right) r dr dz \quad (15)$$

C is a rectangular coupling matrix, can be written as follows:

$$C = \iint X_i \frac{\partial X_j}{\partial r} dr dz \quad (16)$$

and F is the external loading vector.

Equation 11 must be integrated in time. To integrate Equation 11 with respect to time, there are many methods available, but we consider only the simplest linear interpolation in time using finite difference, thus:

$$\begin{aligned} &\theta KMr_1 + \theta Cu_{e1} = (\theta - 1)KMr_\theta + (\theta - 1)Cu_{e0} + F \\ &\theta C^T r_1 - \theta^2 \Delta tKPu_{e1} = \theta C^T r_0 - \theta(\theta - 1)\Delta tKPu_{e0} \end{aligned} \quad (17)$$

In above equations, if $\theta \geq 0.5$, the system will be stable without any condition, in the Crank-Nicolson type of approximation, θ is made equal to 0.5, or in the Galerkin approximation θ is equal to 0.67. By using θ = 0.5 in Crank-Nicolson method, Equation 14 can be written as follows:

$$\begin{bmatrix} KM & C \\ C^T & -\frac{\Delta t}{2} KP \end{bmatrix} \begin{bmatrix} r_{n+1} \\ u_{e_{n+1}} \end{bmatrix} = \begin{bmatrix} -KM & -C \\ C^T & \frac{\Delta t}{2} KP \end{bmatrix} \begin{bmatrix} r_n \\ u_{e_n} \end{bmatrix} + \begin{bmatrix} 2F \\ 0 \end{bmatrix} \quad (18)$$

Therefore values of unknown can be calculated at time $t = t_{n+1}$ based on known parameters at time $t = t_n$. For initial conditions at time $t = 0$ all values are known.

After finding governing matrix equations for a single element, the assembled matrices for total elements can be obtained and boundary conditions can be introduced. Solving such equations at any time, horizontal and vertical deformations (u,v) at various nodal points can be found and strain values for each element can be calculated.

It should be noted that in the above equations parameters such as coefficient of permeability and elasticity are function of time. If the time directly substitute in the above equations the problem would be more complicated. In order to reduce this difficulty of solution the following procedure was performs.

By assuming similar variation of longitudinal and radial coefficient of consolidation, it can be written for cycle N as:

$$T_{vN} = \frac{C_v t'}{H_d^2} \quad (19)$$

In the above equation, t' is function of time, number of cycle and normally and overly coefficient of consolidation.

Therefore by using Equation 20 at the end of each cycle settlement and water pressure can be determine:

$$\begin{aligned} \delta_N &= (1 - \alpha)\delta_{N-1} \\ u_{ecN} &= (1 - \alpha)u_{ecN-1} \end{aligned} \quad (20)$$

Where **a** is the ratio of coefficient of volume change for overly consolidated soil over normally consolidated, **d** and u_e are settlement and pore water pressure respectively.

Vertical effective stress change due to ground water level change

The equivalent external load due to water table decline can be computed from Figure 1. If water table drops to be equal h, then:

$$\begin{aligned} &h = h_1' - h_1 = h_2 - h_2' \\ &\sigma_{v0}' = \gamma_{sand} h_1' + (\gamma_{sat} - \gamma_w) h_2 \\ &\sigma_{v1}' = \gamma_{sand} h_1' + (\gamma_{sat} - \gamma_w) h_2' \\ &\sigma_{v1}' = \gamma_{sand} (h_1 + h_1') + (\gamma_{sat} - \gamma_w)(h_2 - h_1) \\ &\Delta\sigma_v' = \sigma_{v1}' - \sigma_{v0}' = [\gamma_{sat} - (\gamma_{sat} - \gamma_w)]h \end{aligned} \quad (21)$$

where σ'_{v0} = initial vertical effective stress,

σ'_{v1} = final vertical effective stress, and

$\Delta\sigma'_{v}$ = estimated vertical load at top layer of clay.

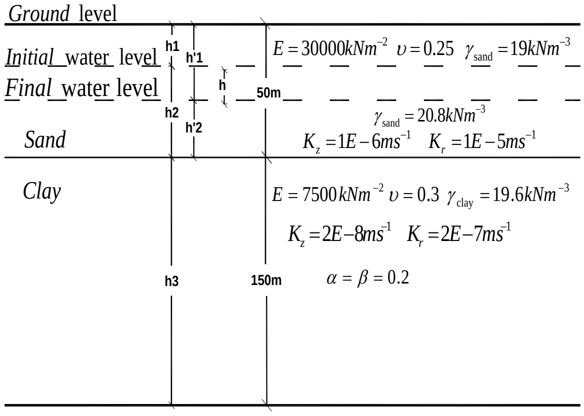

Figure 2: Declined Water Level and Rafsajan Aquifer Soil Profile

Numerical Results

Formulation of finite element analysis for subsidence problem was discussed in previous section. A computer program was developed to predict and examine various soil behavior and conditions under cyclic loading. In order to verify the computer model, analysis for simple behavior such as one-dimensional consolidation was performed. As an example for examination of model, properties of Rafsanjan aquifer in Kerman Province were considered, which is given in Figure 2. It should be noted that values of E and other material properties can be varied in depth or other directions. Values of C_r C_z are functions of K, E, ν, γ and Δt and was chosen from 30 minutes to one day depend on required accuracy and the problem.

A section with height of 200 meters and width of 1000 meters was discretized to 160 rectangular elements with 189 nodes. For complete study two stages of analysis were performed in this research.

At first stage of this study, in order to examine the consolidation process for continuous loading with cyclic loading under elastic condition, it is assumed that water table suddenly drops by about one meter and water flows in axial and radial directions under axi-symmetric conditions. This simulation is very close to actual filed condition under pumping of groundwater through wells. At this conditions water flows in three dimensions and consolidation process and water drainage occur faster than single drainage. The analysis for this case is shown in Figure 3.

It can be seen from Figure 3 that amount of subsidence is higher for continuous loading compare to cyclic loading.

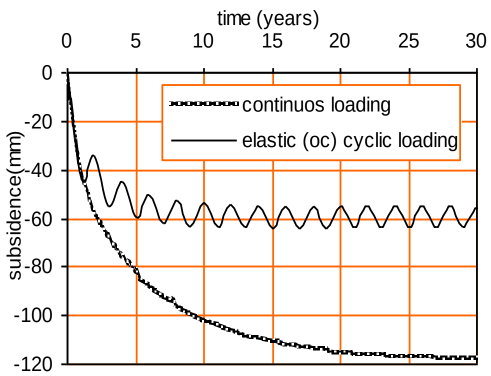

Figure 3: Comparison of Continues Cyclic Consolidation

As explained in section 2 of this paper, by assumption of independent effect of loading on each cycle, this would introduce an error. This error shows negative pore pressure in the next cycle. At the period of no loading if the negative pore water pressure dose not dissipate, this could create an extra compressive effective stress on the system. Therefore, this error would influence on the computing of the final settlement which usually is smaller than the actual settlement. This effect is shown in Figure 4 for cyclic time of 2 years and water table drop of 0.5 meter.

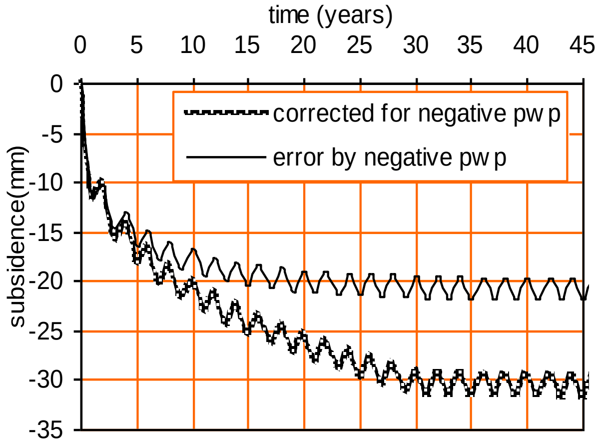

Figure 4: Effect of Negative PWP on No Pumping Cycle and Corrected once

At the second stage of the study relationship between subsidence and time for elastic (oc) and inelastic soil under cyclic loading were developed. It can be seen that the settlement would get equal for both conditions after certain time which only depend on Beta as explained in section 2. Figure 6 shows that the results of subsidence rate vs. time for cyclic period of one year at water table drop of 0.5 and 1 meter. Figure 7 shows that the results of subsidence rate vs. time for cyclic period of one and two years at water table drop of 0.5.

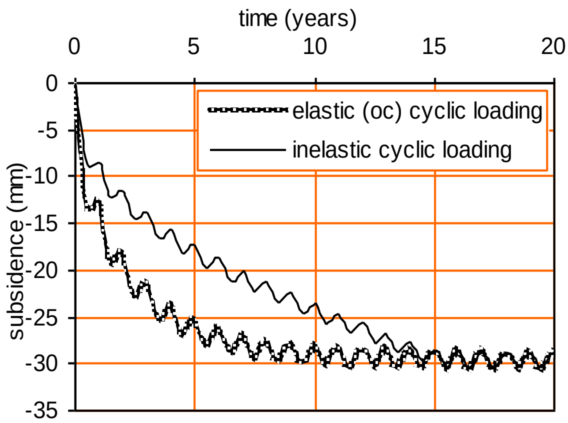

Figure 5: Relationship between Subsidence and Time for Elastic (OC) and Inelastic Cyclic Loading

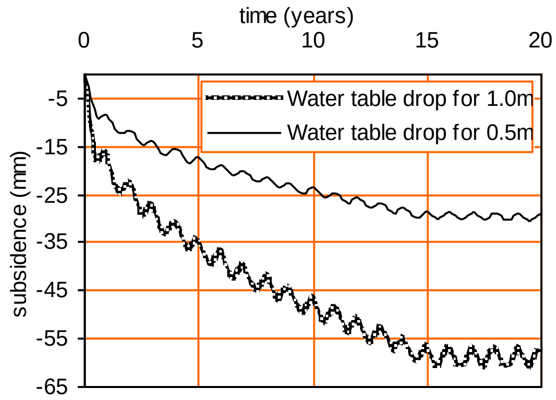

Figure 6: Relationship between Subsidence and Time For Cyclic Period of One Year

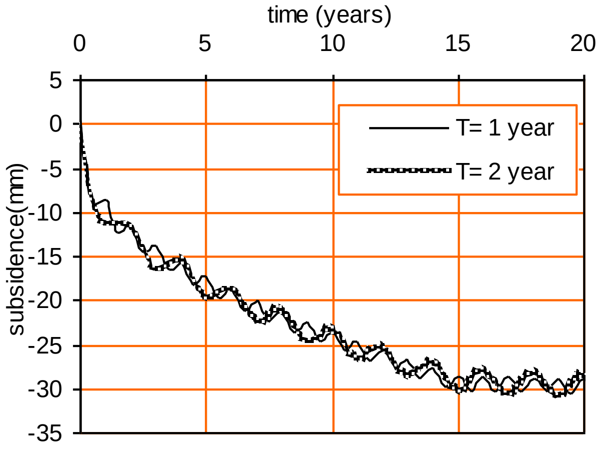

Figure 7: Relationship Between Subsidence and Time for Water Table drop of 0.5 meter

Conclusion

The developed computer program based on Biot's three-dimensional consolidation theory and cyclic loading gave satisfactory results. First, the proposed method was examined with classical and one dimensional consolidation theory and then extend to more complicated causes which still confirmed field data, and finally based on that the prediction of future settlement can be obtained. The limitation of this study is that aquifer was assumed as a confined one. This study first was developed for considering only continuous loading as elastic over consolidated under cyclic loading with about 56% different. Then effect of negative pore water pressure was corrected by special case. It's observed that the different between cycle period of one year and two years is only 3%. This is mainly due to high thickness of clay layer. If this thickness become thin the effect would be higher. Finally, the effects of different variable were examined and satisfactory results were obtained. The models were compared with field data in Rafsanjan basin and good correction between them was observed.

References

[1]. Rahmanian, D. 1986. Land subsidence and earth fissures due to groundwater withdrawal in Kerman, Iranian Journal of Water, 6: pp. 27-40.

[2]. Toufigh, M. M., and Shafiei, B. 1995. Prediction of future land subsidence in Kerman due to ground water withdrawal. 5th International Symposium on Land Subsidence, Netherland.

[3]. Toufigh, M. M., and Shafiei, B. 1996. Finite element consolidation model for subsidence problem based on Biot's three dimensional theory. 1996. Indian Geotechnical Journal, 26(3).

[4]. Toufigh, M. M., and Q'marsi, k. 2002. Single well subsidence modelling based on finite element formulation. Canadian Speciality Conference on computer Application in Geotechniqu. Winnipeg, Manitoba, Canada.

[5]. Ouria, A., and Toufigh, M. M. (2010). "Prediction of land subsidence under cyclic pumping based on laboratory and numerical simulations." J. Geotech. Geol. Eng., 28(2), 165–175.

[6]. Baligh, M.M., and Levadoux, J. 1978. Consolidation theory for cyclic loading. Journal of the Geotechnical Engineering Division, ASCE, 104(4): pp. 415-431.

[7]. Toufigh,M.M., and Ouria, A. (2009). "Consolidation of inelastic clays under cyclic loading." Soil. Dyn. Earthquake Eng., 29(2), 356–363.